Synthetic Metals 216 (2016) 23–30

Contents lists available at ScienceDirect

Synthetic Metals

journal homepage: www.elsevier.com/locate/synmet

Effect of a high boiling point additive on the morphology of solution-processed P3HT-fullerene blends

Yun Long, Alexander J. Ward, Arvydas Ruseckas, Ifor D.W. Samuel*

Organic Semiconductor Centre, SUPA, School of Physics and Astronomy, University of St Andrews, St Andrews, Fife KY16 9SS, United Kingdom

ARTICLE INFO

Article history:
Received 28 October 2015
Accepted 3 December 2015
Available online 25 January 2016

Keywords:
Organic solar cells
OPV
Conjugated polymers
Bulk heterojunction
Fluorescence quenching
Exciton harvesting

ABSTRACT

The use of high boiling point additives in solution processing has been widely employed to control the active layer morphology in bulk heterojunction organic solar cells. The morphology of the heterojunction is crucial in controlling charge separation and extraction by the electrodes, and therefore the power conversion efficiency (PCE) of the device. This paper presents a study of time-resolved fluorescence quenching in blends of P3HT containing varying concentrations of the fullerenes $PC_{61}BM$ or $PC_{71}BM$. The relationship between the fluorescence quenching rate and fullerene concentration indicates that the fullerene molecules are dispersed within the P3HT film for up to 5% by mass of fullerene. For higher fullerene concentrations, the additional fullerene molecules aggregate and form fullerene domains. The high degree of phase segregation observed in these blends is beneficial for solar cell performance because the segregated fullerene phase provides electron percolation pathways through the blend. The addition of 1,8-diiodooctane (DIO) to the solutions for spin coating into films changes the scale of fullerene segregation when the ratio by mass of fullerene exceeds 20%. At high fullerene concentrations the rate of fluorescence quenching decreases in P3HT:$PC_{61}BM$ blends when prepared with DIO indicating a larger scale phase separation. The effect of DIO on the morphology of P3HT:$PC_{71}BM$ blends is the opposite in that it causes faster quenching in the blends. Overall the results show that DIO can be used to control the morphology of photovoltaic blends of P3HT with fullerenes.

1. Introduction

Conjugated polymers are promising materials for solar cells. When incorporated in bulk heterojunction organic photovoltaic devices, they are capable of producing power conversion efficiencies (PCEs) of over 10% [1,2]. Nanocomposite blends consisting of a conjugated polymer and fullerene derivative are often used as active layers which are of great potential for solar cells due to being easily processable from solution. This also allows them to be inexpensively deposited on flexible substrates at low cost. In addition, they are lightweight, have a high absorption coefficient ($\sim 10^5\ cm^{-1}$) and flexible [3–5]. Absorption of light by a conjugated polymer leads to the generation of a bound electron–hole pair known as an exciton, which must be separated into its constituent charges in order to produce an electric current. This is achieved by blending the conjugated polymer – which acts as the donor – with an acceptor of higher electron affinity, such that the electron is then transferred to the acceptor. The dissociation of the exciton occurs at the donor–acceptor heterojunction, so it is important to ensure all light-absorbing sites in the polymer are within reach of the heterojunction. Therefore the morphology of the heterojunction interface coupled with knowledge of the exciton diffusion length (typically on the scale of ~10 nm) [6,7] in the polymer are important parameters in understanding and optimising the rate of charge generation in organic photovoltaic devices.

Exciton dissociation depends on the shape of the donor–acceptor heterojunction interface available to the exciton, which is influenced by the morphology of the active layer within the device structure. In many devices, a donor–acceptor bulk heterojunction is employed in order to be able to optimise the interfacial area [8–11]. To create a bulk heterojunction, the donor and acceptor are dissolved in a solvent, and then deposited onto a substrate to form an intermixed nanocomposite blend with a high surface-area per volume for the interface. The large surface area of the bulk heterojunction bears an advantage over a planar heterojunction, and results in excitons in the donor having an increased chance of encountering the interface. It is also important, however, that within a bulk heterojunction, continuous pathways are maintained such that the separated electron and hole are able to reach the interface before recombination occurs. These factors are considered when optimising the morphology of the bulk heterojunction,

* Corresponding author. Fax: +44 1334463104.
E-mail address: idws@st-and.ac.uk (I.D.W. Samuel).

http://dx.doi.org/10.1016/j.synthmet.2015.12.004

which endeavors to strike a balance between the two by achieving a phase separated interpenetrating bicontinuous network of the donor and acceptor in the blend. In this way, the morphology of the active layer is important in that it determines the rates of exciton diffusion and charge generation within the device. The molecular structure within either the donor or the acceptor phase directly affects light absorption and carrier mobility during the photovoltaic process, whilst the scale of phase separation between the donor and acceptor phases – in which domains are formed from the acceptor phase – controls the surface area of the donor–acceptor interface at which dissociation of the excitons occurs, and the distance excitons need to diffuse to encounter an acceptor [9–12]. Overall, the active layer morphology is seen to crucially impact the performance of the photovoltaic device [9,10,13–15].

Measuring the morphology is challenging due to the small lengthscales encountered. Techniques such as scanning electron microscopy (SEM) and atomic force microscopy (AFM) have previously been employed to measure the nanoscale morphology of polymer thin films [15,16]. Although such methods have successfully probed the nanoscale morphology in film blends of other polymers – such as PTB7 – with fullerene, in the case of P3HT, the possibility of measuring the dimensions of domain networks formed during phase separation is obstructed by the lack of variation in the hardness of the constituent materials. This makes it difficult to distinguish between the donor and acceptor phase and therefore to make a measurement of their dimensions. Therefore attention has turned to searching instead for indirect methods for probing the morphology in a polymer fullerene blend. Research has demonstrated that the active layer morphology is heavily dependent on the processing steps and solvents used during the deposition. Various processing techniques have been developed in order to control and optimise the morphology. One processing method used is thermal annealing, which involves heating of the active layer at a defined temperature (which occurs between 100 and 130 °C for P3HT) for a finite amount of time [17]. Annealing has been observed to induce separation of the donor and acceptor phases, with the latter forming domains of approximately 10 nm [18–21]. It has been shown that thermal annealing leads to an enhancement in the PCE of devices incorporating P3HT-fullerene blends [22], due to crystallisation of the P3HT or to an enhancement in the morphological structure of the film with larger fullerene domains being formed [8,23]. Another method which has been employed is exposure of the deposited active layer to solvent vapors [24,25]. Recent research has focused on additive processing, due to the improvement in power conversion efficiency observed with the inclusion of solvent additives within the film blends [12,26–28]. Processing of films with the addition of 1,8-diiodooctane (DIO) has been noted as a successful method for improving conversion efficiency in a bulk heterojunction solar cell, with an increase in the internal quantum efficiency by a factor of 2 having been observed [15,29,30].

In this paper, time resolved photoluminescence is measured in polymer-fullerene blends of P3HT:$PC_{61}BM$ and P3HT:$PC_{71}BM$, in order to study how the rate of exciton harvesting is affected by an increase in the acceptor concentration. Solar cells with active layers fabricated from P3HT:$PC_{61}BM$ have demonstrated PCEs of up to 5% [12]. This paper uses time-resolved fluorescence to understand the significance of morphology within the polymer fullerene blends on charge generation in the device. The effect of additive processing on the fluorescence is analysed in order to understand how the morphology of the donor-acceptor interface – and therefore the rate of exciton dissociation – is affected.

2. Experimental methods

The materials incorporated within the film blends consisted of P3HT with regio-regularity 91–94% obtained from Rieke Materials (item number 4002-EE), and $PC_{61}BM$ and $PC_{71}BM$ from Solenne. Film samples were prepared by spin-coating solutions onto fused silica substrates. The solutions for spin-coating were made from stock solutions of P3HT (with concentration 20 mg/ml) and of $PC_{71}BM$ and $PC_{61}BM$ (each with concentrations 0.2 mg/ml, 2 mg/ml and 10 mg/ml.) which were prepared in a nitrogen glovebox using anhydrous chlorobenzene. The stock solutions were stirred overnight at 40 °C. To prepare the solutions for spin-coating into films, the volume of P3HT was fixed whilst the amount of fullerene solution was varied. Firstly, films without additive were spun onto clean fused silica substrates. Then 3% by volume of 1-8-diiodooctane (from Sigma–Aldrich) was added to each of the solutions and stirred for 30 min before spin-coating onto a new set of cleaned silica substrates. The deposited films were then dried for 2 h in an evaporator under high vacuum.

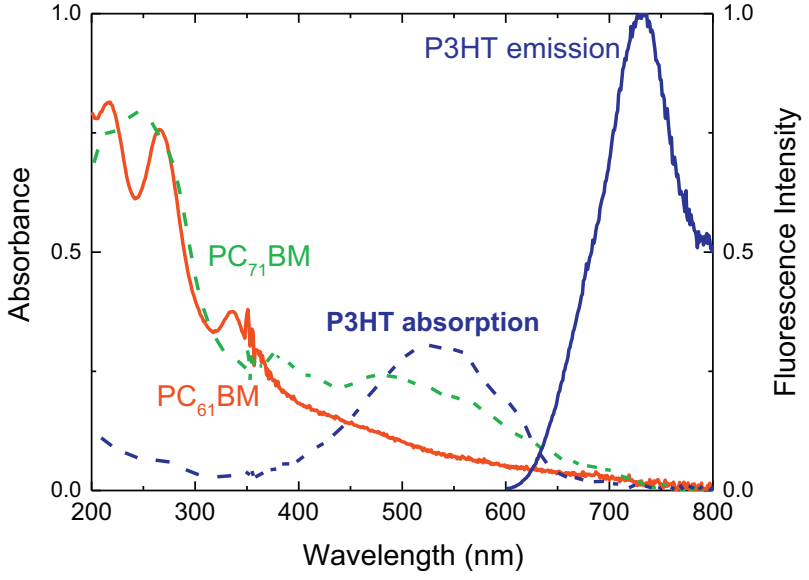

Fig. 1. The absorption spectra for $PC_{71}BM$ (green) and $PC_{61}BM$ (red) and P3HT (dark blue), alongside the fluorescence spectrum for P3HT (in blue). (For interpretation of the references to color in this figure legend, the reader is referred to the web version of this article.).

The films were placed inside a sample chamber under nitrogen, which was sealed inside the glovebox before being removed from the glovebox for measurement. To detect the effect of solvent additives in the blends, the rate of exciton dissociation (quenching) is measured in film blends processed with and without additive. The film samples are optically excited to generate excitons, and the photoluminescence decay of the excitons is measured to give an indication of the rate of exciton dissociation taking place within the blend. The time-resolved photoluminescence of the films was measured using a synchroscan streak camera from Hamamatsu Photonics, giving temporal dynamics from 5 ps to 2 ns. The samples were excited at 400 nm with the frequency doubled output of a Ti: Sapphire oscillator, with a pulse width of 100 fs (FWHM), a repetition rate of 80 MHz and excitation powers kept low (<5 mW) in order to prevent exciton–exciton annihilation caused by comparatively high excitation intensities.

3. Results and discussion

The absorption spectra of P3HT and the fullerenes $PC_{61}BM$ and $PC_{71}BM$ are given in Fig. 1 alongside the steady state fluorescence measured from P3HT. Time-resolved fluorescence measurements of pristine P3HT films (without fullerene) and P3HT blends with increasing amounts of fullerene are shown in Fig. 2 for $PC_{61}BM$ and Fig. 3 for $PC_{71}BM$. For both fullerenes, the fluorescence decay gets faster as the concentration of fullerene rises. The blends prepared with the additive DIO show qualitatively similar results to as-cast blends. The photoluminescence (PL) intensity I is proportional to the density of excitons in P3HT. The measurements were conducted at low excitation densities so that the decay rate of excitons in the pristine film was proportional to the exciton density of a blend.

$$\frac{dI_{\text{pristine}}(t)}{dt} = -kI_{\text{pristine}}(t) \quad (1)$$

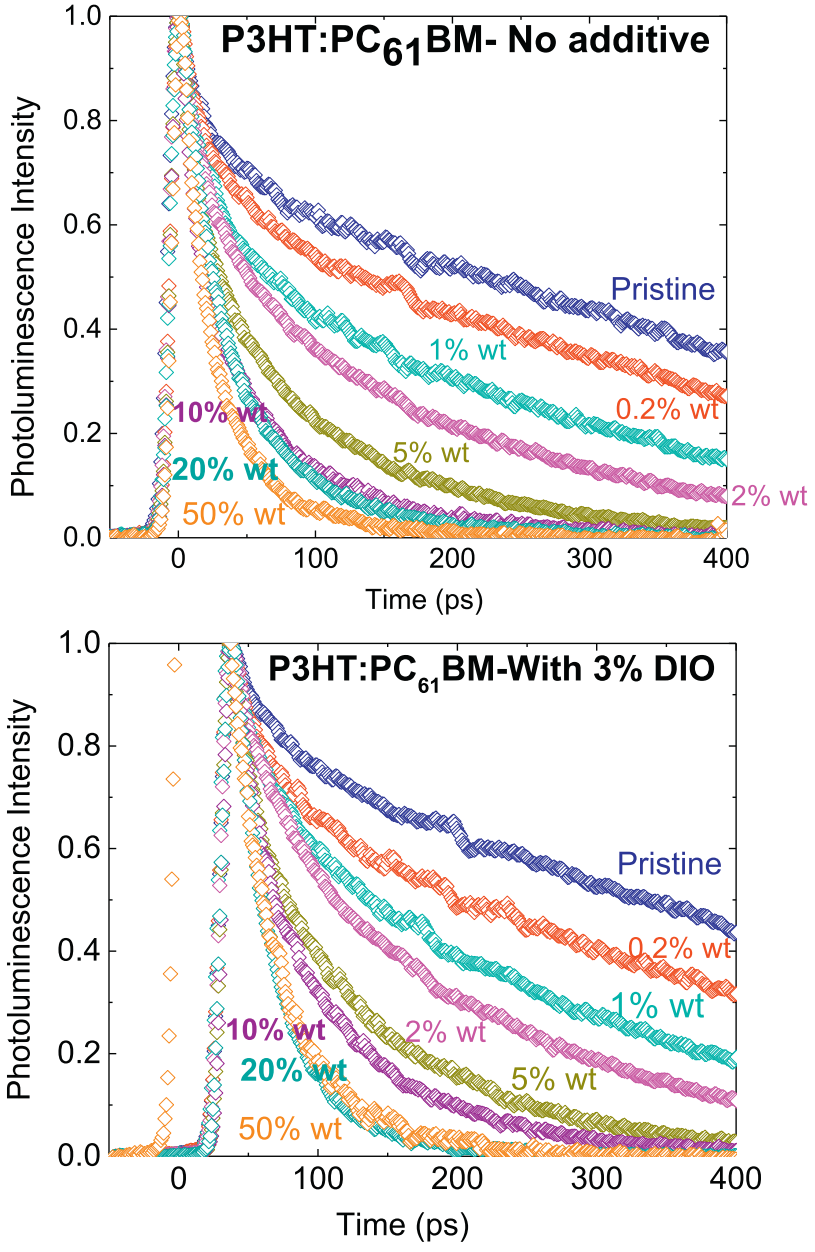

Fig. 2. Normalised time-resolved fluorescence decays obtained from streak camera for blends of P3HT:$PC_{61}BM$ as cast and with additive, comprising ratios of fullerene ranging from 0 to 50% by mass.

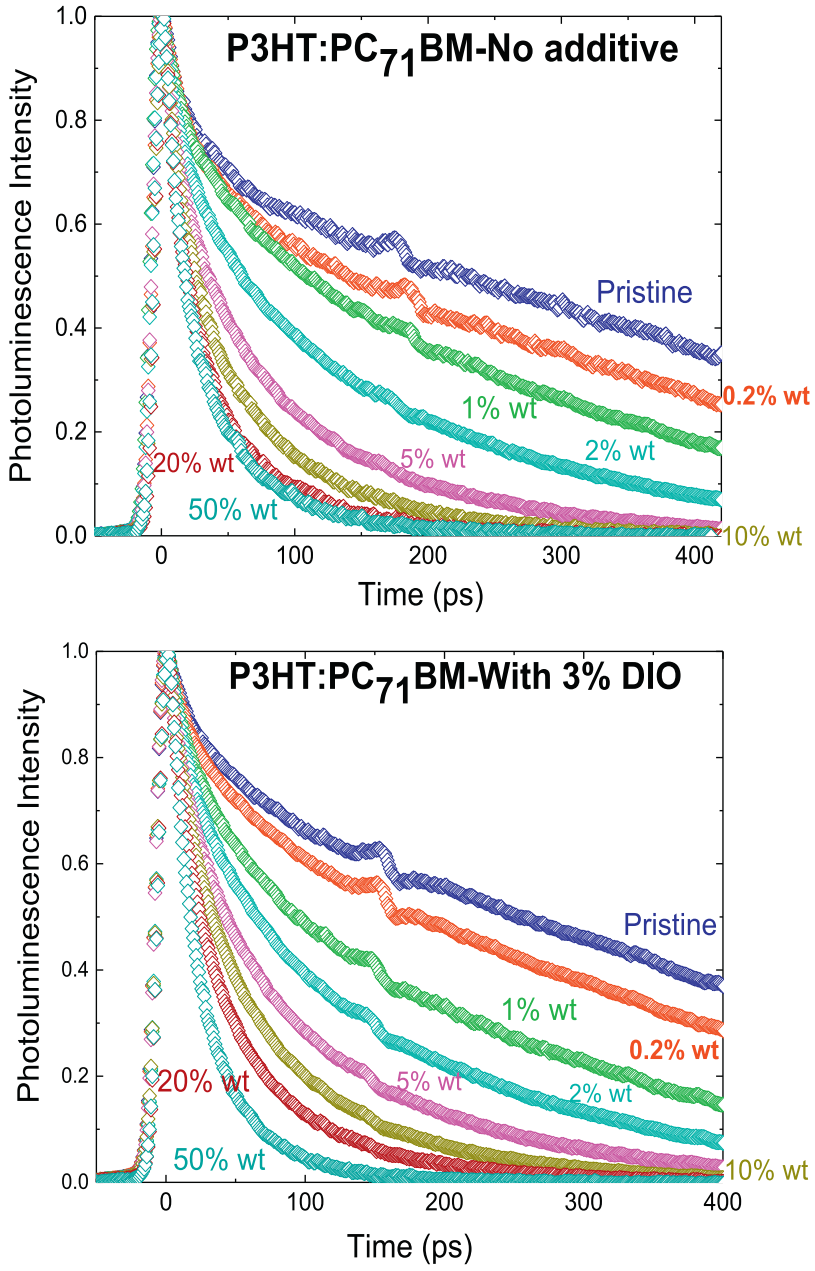

Fig. 3. Normalised time-resolved fluorescence decays obtained from streak camera for blends of P3HT:$PC_{71}BM$ as cast and with additive, comprising ratios of fullerene ranging from 0 to 50% by mass.

Here k is the rate constant for the natural decay of excitons in P3HT film. In the blend there is an additional fullerene—induced decay with a rate constant k_q

$$\frac{dI_{\text{filmblend}}(t)}{dt} = -kI_{\text{filmblend}}(t) - k_q(t)I_{\text{filmblend}}(t) \quad (2)$$

By merging Eqs. (1) and (2) we obtain

$$k_q = -\frac{d}{dt}\left[\ln\left(\frac{I_{\text{filmblend}}}{I_{\text{pristine}}}\right)\right] \quad (3)$$

which shows that the rate constant k_q can be extracted by taking the derivative of the logarithm of the ratio of the PL intensity measured in a blend with fullerene molecules $I_{\text{filmblend}}$ and the PL intensity of a pristine film I_{pristine}. This logarithmic ratio is shown in Fig. 4 for selected blends. At low concentration of the fullerene (2% by weight) the quenching rate is not affected by DIO for both fullerenes. In the blends with a large fraction of $PC_{61}BM$ the addition of DIO slows down the quenching, whereas the opposite effect of DIO is observed for $PC_{71}BM$. The kinetics of the ln(PL ratio) are non-linear at high fullerene content indicating that the rate constant of quenching decreases with time. The kinetics for other fullerene concentrations are shown in the Supplementary information.

Fig. 5 shows the quenching rate constants k_q for as cast and additive processed film blends comprising fullerene concentrations 0–0.45 nm^{-3} (corresponding to mass ratios 0–55%). The values for this plot were obtained by taking the reciprocal of the time τ at which the ln(PL ratio) = −1 ($k_q = 1/\tau$). In film blends with low fullerene concentrations between 0–0.04 nm^{-3} (which correspond to polymer-fullerene mass ratios of 0–5%) the rate constant k_q is proportional to the fullerene concentration N_c. This linear dependence can be interpreted as the fullerene being fully

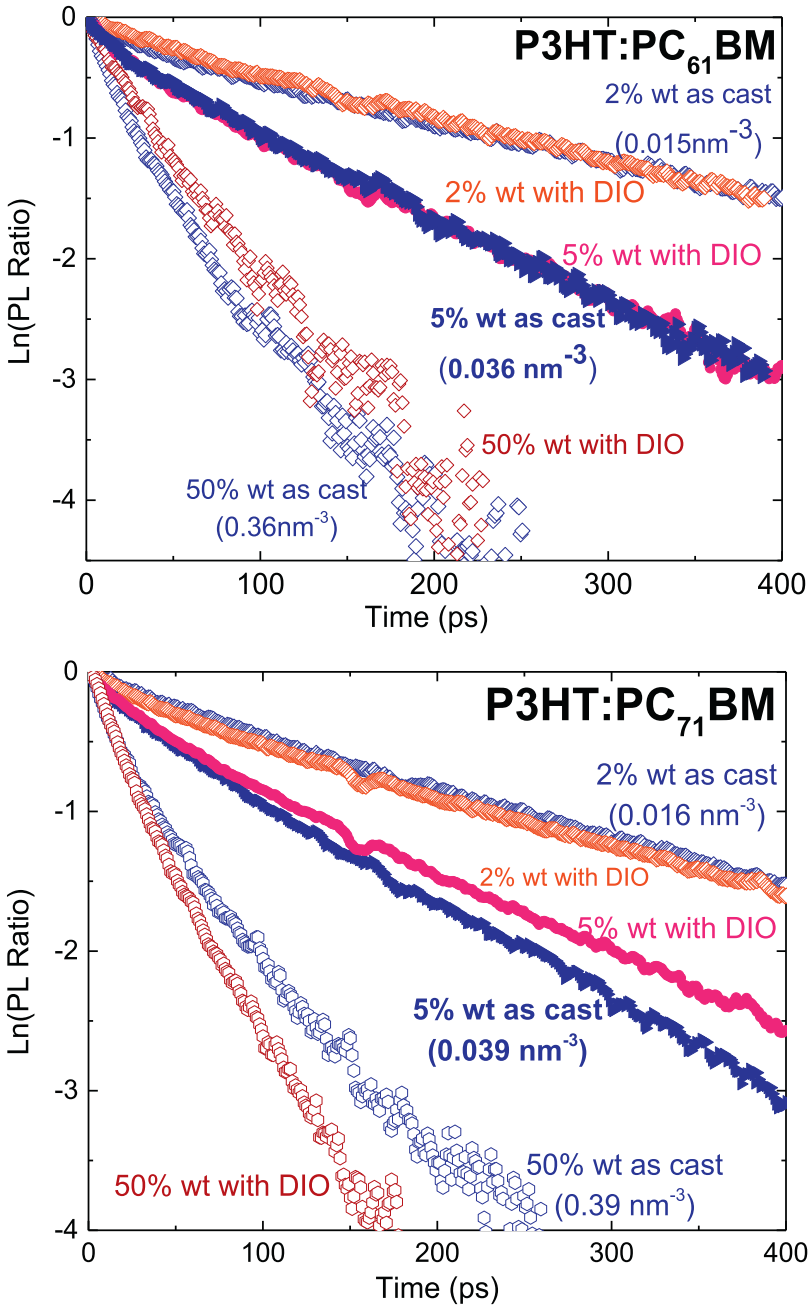

Fig. 4. Logarithm of fluorescence decay ratios in polymer film blends containing polymer- mass ratios of 2%, 5% and 50% by mass of $PC_{61}BM$:P3HT (top) and $PC_{71}BM$:P3HT (bottom).

dispersed throughout the polymer matrix. After the fullerene concentration exceeds 0.04 nm^{-3} (equivalent to a fullerene-polymer mass-ratio of 5%) the increase in the value of k_q becomes sub-linear. This suggests that the fullerene molecules being added to the blend beyond the point of phase segregation do not fully intermix with the polymer. The slower rate at which k_q increases suggests that a segregated phase consisting of pure fullerene has formed from aggregation of these additional fullerene molecules. The aggregation of the fullerene molecules limits the extent of the donor–acceptor interface at which the excitons dissociate as well as controlling the size of the diffusion pathways for the excitons. The segregated phase co-exists alongside the fully intermixed polymer-fullerene. Incorporating the solvent additive DIO into the blend shows an impact on the quenching rate constant k_q for both P3HT:$PC_{61}BM$ and P3HT:$PC_{71}BM$ after the fullerene concentration has exceeded the point of phase separation such that the segregated phase has begun to form. This occurs most noticeably at fullerene concentrations higher than 0.15 nm^{-3} (corresponding to 20% by weight of fullerene). In P3HT:$PC_{61}BM$, the addition of DIO is observed to cause a decrease in k_q, which is attributed to poorer mixing of the fullerene with the polymer than in films of the same composition prepared without DIO, implying that the fullerene domain sizes are larger. In contrast DIO has the opposite effect on k_q in P3HT:$PC_{71}BM$ blends, suggesting a higher degree of mixing in an additive processed film, smaller fullerene domains (see also Figs. S3 and S4 in Supporting information.)

In assuming that the fullerene clusters co-exist with the fully intermixed polymer-fullerene phase, the quenching rate constant k_q is the sum of the rate of exciton quenching by the molecularly dispersed fullerene in the intermixed phase and the rate of

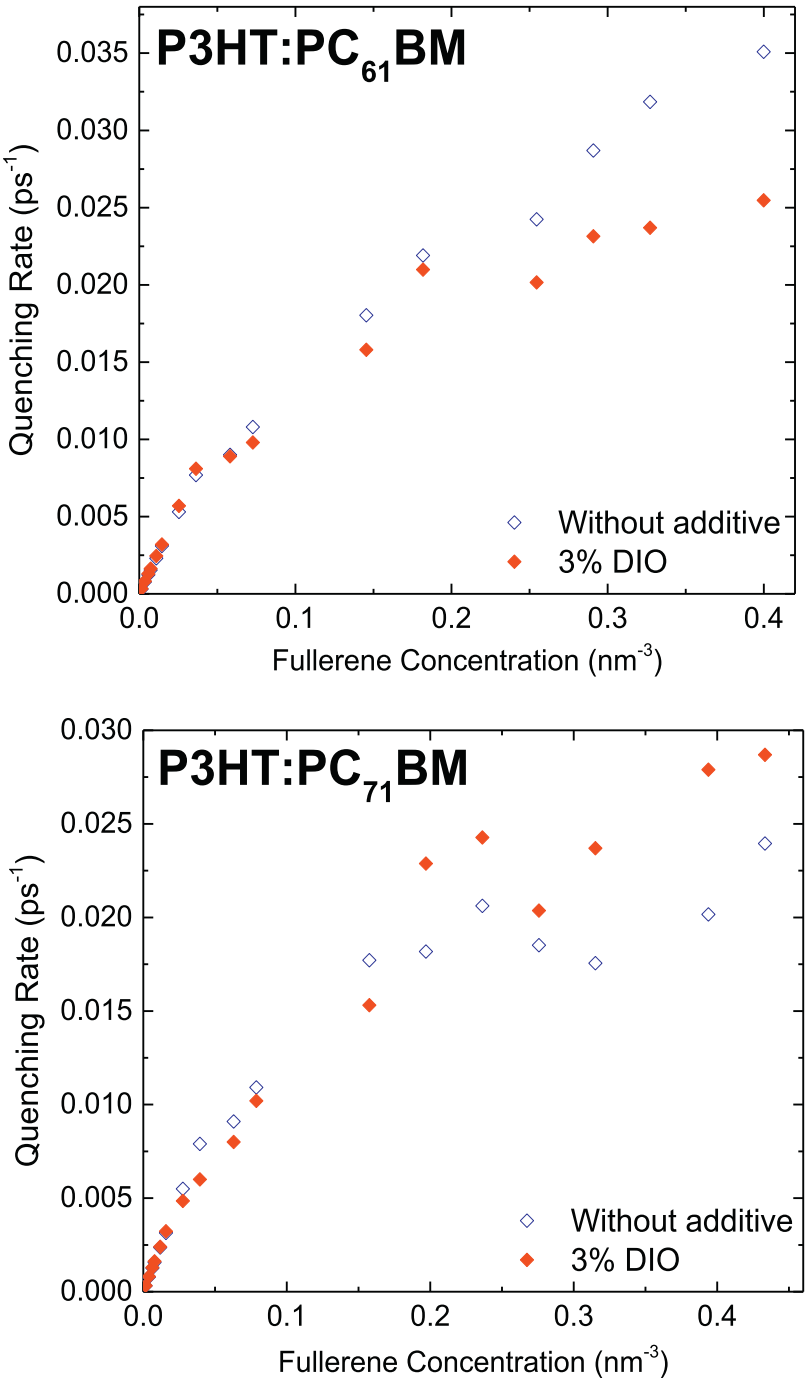

Fig. 5. Quenching rates k_q measured in blends of P3HT doped with $PC_{61}BM$ (top) and $PC_{71}BM$ (bottom), consisting of fullerene concentrations 0–0.45 nm^{-3} (corresponding to ratios-by-mass of 0–55%.) The quenching rates are shown in red for films processed with DIO added and in blue for films without DIO.

quenching of excitons caused by the segregated phase. The results shown in Fig. 5 indicates that exciton quenching in the intermixed phase is not affected by the solvent additive, but in the segregated phase the additive does noticeably affect the quenching rates. This is important for solar cell performance because electrons are likely to get trapped on dispersed fullerene molecules and not extracted to the electrode. In contrast, the segregated fullerene phase can provide the electron percolation pathways through the blend and therefore a high degree of phase segregation is desirable for device performance. Large-scale phase segregation, however, can be detrimental to solar cells because not all excitons would be able to reach an interface between electron donor and acceptor and to generate charge carriers. Many studies have shown that the degree of phase separation and therefore the solar cell performance depends very strongly on the blend morphology.

We can estimate the exciton quenching rate upon an encounter with dispersed fullerene molecules by fitting the PL quenching to the Smoluchowski–Collins–Kimball (SCK) equation which is given in Eq. (4) [31].This equation expresses k_q as a time-dependent function of the exciton capture radius r_c(distance from the centre of a quencher at which an exciton is quenched), the exciton diffusion coefficient D and fullerene concentration N_c. In Eq. (4) k_d is the rate with which the excitons encounter the quencher molecules, whilst k_a is the rate at which they are then quenched.

Table 1
Values of quenching rate at the donor–acceptor interface calculated using the values of k_q shown in Fig. 5 for film blends of mass ratios between 0 and 5%.

Film blend	Quenching rate at interface k_a($nm^3\,ps^{-1}$)
P3HT:PC_{61}BM	0.219 ± 0.010
P3HT:PC_{71}BM	0.232 ± 0.011

The Smoluchowski–Collins–Kimball equation is used to estimate $k_d = 4\pi r_c D$ with the previously reported values $r_c = 1$ nm for PCBM molecules in P3HT matrix and the diffusion coefficient $D = 1.8 \times 10^{-3}\,cm^{-2}\,s^{-1}$ in P3HT [7,32]. This produces a value of $k_d = 2.3\ nm^{-3}ps^{-1}$. The finite rate of quenching at the interface k_a is obtained from fitting the quenching rate k_q for blends with fullerene concentrations of ~0–0.04 nm^{-3} to the SCK equation (fittings are given in Figs. S1 and S2 of Supporting information) while the fullerene molecules are fully dispersed in the polymer matrix. The calculated values of k_a for both PC_{61}BM and PC_{71}BM are given in Table 1 with $k_a = 0.219 \pm 0.010\ nm^3ps^{-1}$ for PC_{61}BM molecules dispersed in P3HT and $k_a = 0.232 \pm 0.011\ nm^3ps^{-1}$ for PC_{71}BM in P3HT.

$$k_q = \frac{k_a N_c}{k_a + k_d}\left(\frac{\frac{4k_a r_c^2}{k_a + k_d}\sqrt{\frac{k_d}{t}} + k_d + \frac{(k_a + k_d)^2 D}{(k_d)^2 r_c^2} \times \frac{k_a \pi^2 r_c^4 \mathrm{ERFC}\left(\frac{(k_a + k_d)\sqrt{Dt}}{k_d r_c}\right)}{(k_a + k_d)^2}}{+ \frac{16\mathrm{Dexp}\left(\frac{(k_a + k_d)^2 Dt}{(k_d)^2 r_c^2}\right) k_a \pi^2 r_c^4}{(k_a + k_d)^2} \times \frac{2}{\sqrt{\pi}} \exp\frac{(k_a + k_d)^2 Dt}{k_d^2 r_c^2}}\right) \quad (4)$$

The fact that k_a is smaller by an order of magnitude than the encounter rate k_d predicted by a diffusion-limited model indicates that the PL quenching is not diffusion-limited. In semi-crystalline P3HT excitons funnel into the crystalline phase much faster before they get quenched by dispersed fullerene molecules. Once excitons are in the crystalline phase their quenching rate k_q is much lower than predicted by a diffusion-limited model for dispersed quenchers. This suggests that the fullerene molecules are expelled from the crystalline P3HT phase. These photophysical findings are consistent with findings by XRD measurements carried out on film blends of P3HT with PCBM, suggesting that fullerene is not present within the crystalline P3HT phase [33–35].

4. Conclusion

A detailed study of time-resolved fluorescence quenching in P3HT blends with PC_{61}BM and PC_{71}BM fullerenes was carried out, with the observations being used to learn about the morphology of blends with varying fullerene concentration. It was observed in blends with up to 5% by weight of fullerene, that the polymer and fullerene were intermixed, but at higher fullerene concentrations, the additional fullerene formed a segregated phase of its own. The high degree of phase segregation observed in these blends is beneficial for solar cell performance because the segregated fullerene phase can provide electron percolation pathways through the blend and so is desirable for device performance.

The effect of the additive DIO on exciton dissociation in the blend was also investigated through observing its effect on fluorescence quenching. It was observed that the use of DIO to prepare blends of P3HT:PC_{61}BM caused slower quenching of the excitons suggesting the formation of larger fullerene domains than in blends prepared without DIO. In contrast, when P3HT is blended with PC_{71}BM (beyond the point of phase separation) exciton quenching becomes faster, suggesting better mixing and smaller domains. Overall these results show that the addition of DIO to the solution used for spin-coating into the films can be used to control the rate of fluorescence quenching and the morphology inside photovoltaic blends. We also showed that the exciton quenching rate in P3HT by dispersed fullerene molecules is an order of magnitude lower than predicted by a diffusion-limited model for dispersed quenchers, suggesting that there is no fullerene in the crystalline P3HT phase.

Acknowledgements

We are grateful to the Engineering and Physical Sciences Research Council of the UK for financial support through grants EP/L505079/1, EP/G03673X/1 and EP/J009016/1. We are also grateful to The European Research Council of the European Union for support through grant 321305.

Appendix A. Supplementary data

Supplementary data associated with this article can be found, in the online version, at http://dx.doi.org/10.1016/j.synthmet.2015.12.004. Further research data supporting this paper can be accessed at http://dx.doi.org/10.17630/298ab909-e527-4408-84af-6fcfbe859dea.

References

[1] L. Dou, J. You, J. Yang, C.-C. Chen, Y. He, S. Murase, T. Moriarty, K. Emery, G. Li, Y. Yang, Nat. Photonics 6 (2012) 180–185.
[2] Y. Liu, J. Zhao, Z. Li, C. Mu, W. Ma, H. Hu, K. Jiang, H. Lin, H. Ade, H. Yan, Nat. Commun. 5 (2014) 1–8.
[3] K.M. Coakley, M.D. McGeehee, Conjugated polymer photovoltaic cells, Chem. Mater. 16 (2004) 4533–4542.
[4] S. Ito, H. Ohkita, H. Benten, S. Honda, Spectroscopic analysis of NIR-dye sensitization in bulk heterojunction polymer solar cells, In Ambio (2012) p132–p134.
[5] W. Cai, X. Gong, Y. Cao, Solar Energy Mater. Solar Cells 94 (2009) 114–127.
[6] S.M. Menke, R.J. Holmes, Energy. Environ. Sci. 7 (2014) 469–512.
[7] P.E. Shaw, A. Ruseckas, I.D.W. Samuel, Adv. Mater 20 (2008) 3516–3520.
[8] D. Chirvase, J. Parisi, J.C. Hummelen, V. Dyakonov, Nanotechnology (2004) 1317–1323.
[9] Y. Yao, J. Hou, X. Zheng, G. Li, Y. Yang, Adv. Funct. Mater. (2008) 1783–1789.
[10] T.L. Benanti, D. Venkataraman, Photosyn. Res. 87 (2005) 73–81.
[11] J.J.M. Halls, C.A. Walsh, N.C. Greenham, E.A. Marseglia, R.H. Friend, S.C. Moratti, Nat. Commun. 376 (1995) 498–500.
[12] N. Abu-Zahra, M. Algazzar, J. Solar Energy Eng. 136 (2014) 021023-1-7.
[13] J.W. Jung, J.W. Jo, C. C-C, F. Liu, H.-J. Won, T.-P. Russell, A.K.Y. Jen, Adv. Mater. (2015) 3310–3317.
[14] F. Liu, Y. Gu, J.W. Jung, W.H. Jo, J. Polym. Sci. 50 (2012) 1018–1044.
[15] G.J. Hedley, A.J. Ward, A. Alekseev, C.T. Howells, E.R. Martins, L.A. Serrano, G. Cooke, A. Ruseckas, I.D.W. Samuel, Nat. Commun. 4 (2013) 1–10.
[16] H. Hoppe, M. Niggemann, C. Winder, J. Kraut, R. Hiesgen, A. Hinsch, A. Meissner, N.S. Sariciftci, Adv. Funct. Mater. 14 (2004) 1005–1011.
[17] J. Jo, S.-S. Kim, S.-I. Na, B.-K. Yu, D.-Y. Kim, Adv. Funct. Mater. 19 (2009) 866–874.
[18] R.A. Marsh, J.M. Hodgkiss, S. Albert-Seifred, R.H. Friend, Nanoletters (2010) 923–930.
[19] H. Wang, H.-Y. Wang, B.-R. Gao, L. Wang, Z.-Y. Yang, X.-B. Du, Q.-D. Chen, J.-F. Song, H.-B. Sun, Nanoscale 3 (2010) 2280–2285.
[20] L.F. Drummy, R.J. Davis, D.L. Moore, M. Durstock, R.A. Vaia, J.W.P. Hsu, Chem. Mater. (2011) 907–912.
[21] U. Zhokhavets, T. Erb, H. Hoppe, G. Gobsch, N.S. Sariciftci, Thin Solid Films (2006) 679–682.
[22] F. Padinger, R.S. Rittberger, N.S. Sariciftci, Adv. Funct. Mater. 13 (2015) 85–88.
[23] H. Chen, J. Mater. Chem. A 1 (2013) 5309.
[24] H. Tang, G. Lu, L. Li, J. Li, Y. Wang, X. Yang, J. Mater. Chem 20 (2010) 683–688.
[25] L. Gang, Y. Yao, H. Yang, V. Shrotriya, G. Yang, Y. Yang, Adv. Funct. Mater. (2007) 1636–1644.
[26] J.K. Lee, W.L. Ma, C.J. Brabec, J. Yuen, J.S. Moon, J.Y. Kim, K. Lee, G.C. Bazan, A.J. Heeger, J. Am. Chem. Soc. 130 (2007) 3619–3623.
[27] J. Peet, J.Y. Kim, N.E. Coates, W.L. Ma, D. Moses, A.J. Heeger, G.C. Bazan, Nat. Mater. 6 (2007) 497–500.
[28] J.T. Rogers, K. Schmidt, M.F. Toney, G.C. Bazan, E.J. Kramer, JACS 134 (2012) 2884–2887.
[29] X. Fan, S. Zhao, C. Yue, Q. Yang, W. Gong, Y. Chen, H. Wang, Q. Jia, Z. Xu, X. Xu, J. Nanosci. Nanotechnol. 14 (2014) 3592–3596.

[30] A. Solanki, B. Wu, T. Salim, Y.M. Lam, T.C. Sum, Phys. Chem. Chem. Phys. 17 (2015) 26111–26120.
[31] F.C. Collins, G.E. Kimball, Diffusion controlled reaction rates, J. Colloid Sci. 4 (1949) 425–437.
[32] A. Ruseckas, P.E. Shaw, I.D.W. Samuel, Dalton Trans. (2009) 10040–10043.
[33] A.C. Mayer, M.F. Toney, S.R. Scully, J. Rivnay, C.J. Brabec, M. Scharber, M. Koppe, M. Heeney, I. McCulloch, M. McGeehee, Adv. Funct. Mater. 19 (2009) 1173–1179.
[34] W. Ma, C. Yang, X. Gong, K. Lee, A.J. Heeger, Adv. Funct. Mater. 15 (2005) 1617–1622.
[35] M. Koppe, M. Scharber, C. Brabec, W. Duffy, M. Heeney, I. McCulloch, Adv. Funct. Mater. 17 (2007) 1371–1376.